Journal of Biological Dynamics

ISSN: 1751-3758 (Print) 1751-3766 (Online) Journal homepage: http://www.tandfonline.com/loi/tjbd20

Prion dynamics with size dependency–strain phenomena

V. Calvez , N. Lenuzza , M. Doumic , J-P Deslys , F. Mouthon & B. Perthame

To cite this article: V. Calvez , N. Lenuzza , M. Doumic , J-P Deslys , F. Mouthon & B. Perthame (2010) Prion dynamics with size dependency–strain phenomena, Journal of Biological Dynamics, 4:1, 28-42, DOI: 10.1080/17513750902935208

To link to this article: http://dx.doi.org/10.1080/17513750902935208

Journal of Biological Dynamics
Vol. 4, No. 1, January 2010, 28–42

Prion dynamics with size dependency–strain phenomena

V. Calvez[a†], N. Lenuzza[b,e†], M. Doumic[c], J-P Deslys[b], F. Mouthon[b‡] and B. Perthame[c,d‡*]

[a] *UMPA, ENS-Lyon, 46, allée d'Italie, 69000 Lyon, France;* [b] *CEA-Institute of Emerging Diseases and Innovative Therapies, Route du Panorama, Bat. 60, 92265 Fontenay-aux-Roses, France;* [c] *INRIA Paris-Rocquencourt, Bang, BP105, 78153 LeChesnay Cx, France;* [d] *UPMC-Paris 6, Laboratoire J.-L. Lions, BC187, 4, pl. Jussieu, 75252 Paris Cx 05, France;* [e] *Ecole Centrale Paris, Laboratoire MAS, Grandes Voies des Vignes, 92295 Chatenay-Malabry, France*

(*Received 23 October 2008; final version received 15 March 2009*)

Models for the polymerization process involved in prion self-replication are well-established and studied [H. Engler, J. Pruss, and G.F. Webb, *Analysis of a model for the dynamics of prions II*, J. Math. Anal. Appl. 324 (2006), pp. 98–117; M.L. Greer, L. Pujo-Menjouet, and G.F. Webb, *A mathematical analysis of the dynamics of prion proliferation*, J. Theoret. Biol. 242 (2006), pp. 598–606; J. Pruss, L. Pujo-Menjouet, G.F. Webb, and R. Zacher, *Analysis of a model for the dynamics of prions*, Discrete Cont. Dyn. Sys. Ser. B 6(1) (2006), pp. 215–225] in the case where the dynamics coefficients do not depend on the size of polymers. However, several experimental studies indicate that the structure and size of the prion aggregates are determinant for their pathological effect. This motivated the analysis in Calvez *et al.* [*Size distribution dependence of prion aggregates infectivity*, Math Biosci. 217 (2009), pp. 88–99] where the authors take into account size-dependent replicative properties of prion aggregates.

We first improve a result concerning the dynamics of prion aggregates when a pathological state exists (high production of the normal protein). Then we study the strain phenomena and more specifically we wonder what specific replicative properties are determinant in strain propagation. We propose to interpret it also as a dynamical property of size repartitions.

Keywords: prion kinetics; polymerization process; size repartition; duality method; strain phenomena

MSC Subject Classification: 35B35; 45K05; 92C45

1. Introduction

The prion protein is known to be at the origin of fatal neurodegenerative diseases as Creutzfeldt–Jakob disease (CJD) in human and bovine spongiform Encephalopathy in cattle. Even though the detailed mechanism remains mostly unclear, a largely accepted hypothesis suggests the infectious agent is the misfolded form (called PrPsc) of the normal prion protein (PrPc). According to this protein-only hypothesis, abnormal PrPsc can convert PrPc by a still unknown autocatalytic process [20,29]. Very intringuing in this context is that prion infectious agent can exist under different

*Corresponding author. Email: Benoit.Perthame@upmc.fr
†These authors contributed equally to this work.
‡These authors contributed equally to supervise this work.

ISSN 1751-3758 print/ISSN 1751-3766 online

DOI: 10.1080/17513750902935208
http://www.informaworld.com

strains. Prion strains have been initially distinguished by incubation periods and lesion profiles in congenic mice [4,14]. Nowadays, a large body of literature suggests that differences between prion strains lie in the diversity of PrPsc structure, that can be stably and faithfully propagated (see [8,25] for reviews). However, it remains poorly understood how these changes in the PrPsc conformation can account for their physiopathological effects [21]. Moreover, transmission of prion diseases between different mammalian species is almost systematically less efficient than within a single species [8]. This obstruction has been termed species barriers. Early studies argue that this barrier resides in the PrP primary structure difference between donor and recipient species [28]. However, BSE strain capability confirmed that different strains propagated in the same host may have completely different barriers to another species. Consequently, transmission barrier appears to depend on prion strain specificities [4,9]. A critical challenge of prion biology consists in understanding how a diversity of strains may exist in the same host (expressing the same PrP molecule) and what structural basis of prion strains determines the strength of the species barrier.

As for many protein misfolding disorders (Alzheimer's disease, Parkinson's disease and many other), misfolded PrPsc has the ability to polymerize and form long aggregates called fibrils. Fibrils can be observed while the transconformation process arises at time and size scales mostly unaccessible to experiments. This is why mathematical models are useful to forecast consequences of modelling assumptions at that scale. Based on fibrilar aggregation, the model which seems by now broadly accepted is the one of nucleated polymerization. In this approach, PrPsc is considered to be a polymeric form of PrPc. Polymers can lengthen by addition of PrPc monomers, and they can replicate by splitting into smaller fragments [12,15,30]. It is worth noting that this model leads to an unimodal size distribution of PrP aggregates, which seems to be quite insensitive to small variations of parameters [31]. Greer *et al*. [16] recently improved the model and include a mean saturation effect by the whole population of polymers onto the lenghtening process (called general incidence), and polymer joining (through a Smoluchowski coagulation equation). In all these models, each aggregate has the same behaviour, regardless of its size. However, recent experimental analysis of relation between infectivity and size distribution of PrPsc aggregates (for PrPsc purified from infected brain [33] or for PrPsc produced by PMCA [38,39], a technique which alternates PrPsc aggregates' growth during incubation phases and aggregates' fragmentation during sonication phases) contradicts this uniform behaviour of PrPsc aggregates. In addition, some complexity in the PrPsc aggregate size distribution is more likely to occur within the real process [33]. This leads to consider a model which can reproduce such a behaviour, and the simplest modelling assumption consists in introducing extension rates that depend on the fibril size [6].

This motivates to use the following model for prion polymerization where $V(t)$ denotes the quantity of PrPc (normal protein), $x \in (0, +\infty)$ denotes the size of aggregates and $u(x,t)$ the density of aggregates of size x,

$$\begin{aligned}
&\frac{\mathrm{d}V(t)}{\mathrm{d}t} + V(t)\left[\gamma + \int_0^\infty \tau(x)u(x,t)\,\mathrm{d}x\right] = \lambda,\\
&\frac{\partial u(x,t)}{\partial t} + V(t)\frac{\partial}{\partial x}\big(\tau(x)u(x,t)\big) + [\mu(x)+\beta(x)]u(x,t) = 2\int_x^\infty \beta(y)\kappa(x,y)\,u(y,t)\,\mathrm{d}y,\\
&u(0,t) = 0,
\end{aligned} \tag{1}$$

together with appropriate initial conditions (u^0, V^0). This is a well-established family of models used for describing aggregation, fragmentation in polymers as well as natural production of monomers $V(t)$ (possibly already small aggregates of PrPsc molecules) [12,15,16,19,30,34]. Compared to earlier completely discrete models, it has the advantage of taking into account two scales, as depicted by Figure 1; (i) a small scale (of the order of several PrPsc molecules) for

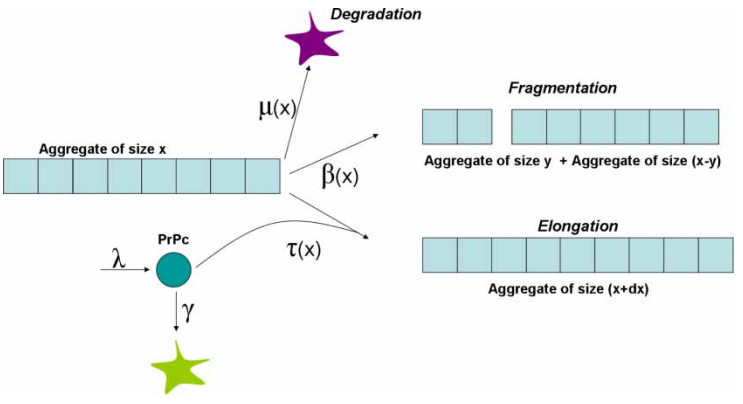

Figure 1. Kinetic model of the prion aggregate growth model based on Figure 2 of Masel *et al.* [22].

continuous aggregation represented by the x-derivative and (ii) a large scale for the total length of the fibrils represented by the integral term. It can be derived through an asymptotic analysis departing from the single PrPsc scale with a discrete model [11,13,18].

Well-posedness, in the class of weak solutions, has been studied in great generality by Laurençot and Mischler [19] and Simonett and Walker [34]. Strong solutions to Equation (1) are built by [12] in the case of 'constant coefficients', i.e., where τ, μ are constants, $\beta(x) = \beta_0 x$ and $\kappa(x, y) = 1/y\mathbf{1}_{(0\le x\le y)}$.

The transport term accounts for the growth in size of polymers: their size grows with the rate $V(t)\tau(x)$, proportional to the available PrPc molecules $V(t)$, with an aggregation ability depending on the size of the polymer (a conceivable hypothesis being that their size confers them a peculiar geometry affecting the autocatalytic process). The fragmentation rate, for a polymer of size y, is $\beta(y) > 0$. The repartition of the two fragments of (smaller) sizes x and $y - x$ is given by $\kappa(x, y) \ge 0$. It should thus satisfy the two usual laws [26] expressing that the number of fragments increases but with constant total molecular mass (recall the factor 2 on the right hand side of Equation (1)):

$$\int_0^y \kappa(x, y)\,\mathrm{d}x = 1, \quad \int_0^y x\kappa(x, y)\,\mathrm{d}x = \frac{y}{2}. \tag{2}$$

This implies that this dynamical system is equipped with two natural balance laws

$$\begin{aligned} \frac{\mathrm{d}}{\mathrm{d}t}\int_0^\infty u(x,t)\,\mathrm{d}x &= \int_0^\infty [\beta(x) - \mu(x)]u(x,t)\,\mathrm{d}x, \\ \frac{\mathrm{d}}{\mathrm{d}t}\left(V(t) + \int_0^\infty x\,u(x,t)\,\mathrm{d}x\right) &= \lambda - \gamma V(t) - \int_0^\infty x\mu(x)u(x,t)\,\mathrm{d}x. \end{aligned} \tag{3}$$

In this study, we aim to continue the work initiated in [6]. Amongst other things, a convincing mathematical model has to reproduce the unusual kinetics of PrPsc accumulation and to be compatible with the strain phenomenon.

In Section 2, we address the first question. PrPsc accumulation in brain follows an exponential growth until the death, whereas it invariably reaches a plateau concentration in tissues outside the central nervous system [3,17]. Thus, the mathematical system must have at least two steady states (one corresponding to the healthy state, and one corresponding to the infection). The question of the existence and the stability of these steady states has been extensively studied in the case of 'constant coefficients' in [12,15,16,30]. Here, as in [6,10,11], we are interested in non-constant

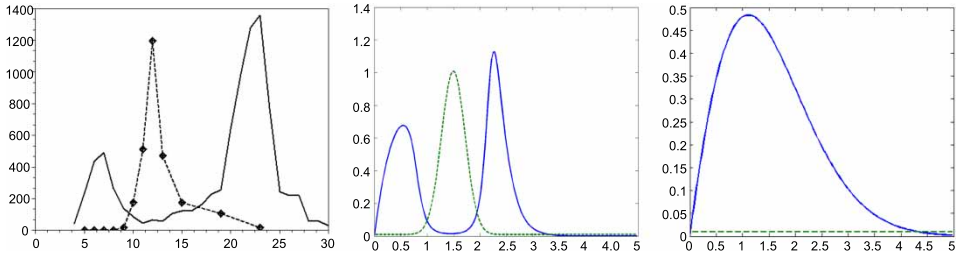

Figure 2. Left: experimental analysis of PrPsc aggregates (data have been kindly provided by J.R. Silveira. For details, see [33]). Size-distribution of PrPsc aggregates in a whole infected hamster brain (solid line) and relative-specific infectivity of each fraction containing PrPsc aggregates with respect to their size (dotted line). The former corresponds to the quantity $xu(x,t)$, and the latter represents a bell-shaped converting rate $\tau(x)$. These are, however, undirect measurements after purification and sonication (i.e. fragmentation induced by ultrasound). Centre: size distribution obtained by solving numerically Equation (6) for a suitable bell-shaped converting rate $\tau(x)$ (dotted line), the non-zero steady state solution presents a bimodal shape (solid line). Right: size distribution corresponding to 'constant coefficients' in model (1).

rates. In such case, the attractivity of the healthy steady state is proved in [6] when λ is small and the infectious steady state does not exist. When the infectious steady state exists, it is not known if it is attractive or if other dynamics such as periodic solutions can exist. Although oscillations are not expected to occur according to experiments, and have not been observed in numerical simulations so far, we are not able to exclude them at the moment. Our first purpose is to give an improved estimate showing that $(u \equiv 0, V = \overline{V})$ is repulsive in the infectious case.

The second question concerning strain mechanism is addressed in Section 3. Our purpose is to indicate a route to study possible relations between PrPsc aggregate size distributions as obtained from the model (1) with 'non-constant coefficients' (especially non-constant elongation rate τ) and the strain phenomena described previously. It is based on the dynamical capability of this nonlinear system to generate size repartitions with high complexity and specific properties, notably the bimodal repartition depicted in Figure 2.

2. Mathematical results

2.1. *Description of the associated eigenproblem*

The eigenproblem associated with the aggregation–fragmentation equation in (1) is useful for the mathematical analysis. For a given $\mathbf{V} > 0$, we denote by $\Lambda(\mathbf{V})$ the first eigenvalue and by $(U(\mathbf{V};x), \varphi(\mathbf{V};x))$ resp. the eigenfunction and the adjoint eigenfunction, that are the solutions to

$$\begin{aligned}
&\mathbf{V}\frac{\partial}{\partial x}(\tau(x)\mathcal{U}(\mathbf{V};x)) + (\mu(x)+\beta(x))\,\mathcal{U}(\mathbf{V};x) - 2\int_x^\infty \beta(y)\kappa(x,y)\mathcal{U}(\mathbf{V};y)\,\mathrm{d}y \\
&\quad = \Lambda(\mathbf{V})\,\mathcal{U}(\mathbf{V};x), \\
&\mathcal{U}(\mathbf{V};0) = 0, \quad \mathcal{U}(\mathbf{V};x) \geq 0, \quad \int_0^\infty \mathcal{U}(\mathbf{V};x)\,\mathrm{d}x = 1. \qquad (4)\\
&-\mathbf{V}\tau(x)\frac{\partial}{\partial x}\varphi(\mathbf{V};x) + (\mu(x)+\beta(x))\,\varphi(\mathbf{V};x) - 2\int_0^x \beta(x)\kappa(y,x)\varphi(\mathbf{V};y)\,\mathrm{d}y \\
&\quad = \Lambda(\mathbf{V})\varphi(\mathbf{V};x), \\
&\varphi(\mathbf{V};x) \geq 0, \quad \int_0^\infty \mathcal{U}(\mathbf{V};x)\varphi(\mathbf{V};x)\,\mathrm{d}x = 1. \qquad (5)
\end{aligned}$$

We remind the reader that the former (4) defines the (opposite of) Malthusian factor $\Lambda(\mathbf{V})$, and expresses the fact that whenever the level of PrPc $\mathbf{V}$ is fixed the population of aggregates grows with the exponential rate $\exp(-\Lambda(\mathbf{V})t)$ and with the asymptotic size-distribution $\mathcal{U}(\mathbf{V}; x)$ (see [23] and comments below for further discussion related to the stationary states). The latter (5) has less clear biological interpretation however. It can be viewed as the natural measure that yields an effective mass conservation for the corresponding aggregation–fragmentation Markov process [26].

Although the solutions of Equations (4) and (5) come formally from the Krein–Rutman theorem, the lack of compactness in the problem requires some specific proof (and technical assumptions on the coefficients). In particular, we shall pay much attention to the competition between the growth term $\partial_x(\tau(x)\mathcal{U}(x))$ which pushes the distribution away from small sizes and the fragmentation term $\beta(x)\mathcal{U}(x) - 2\int_x^\infty \beta(y)\kappa(x, y)\mathcal{U}(y)\,\mathrm{d}y$ which drives the distribution back to small sizes. We refer the interested reader to [10] for existence and assume throughout this paper that the coefficients satisfy the following main conditions:

$$\int_0^x \kappa(z, y)\,\mathrm{d}y \le C\left(\frac{x}{y}\right)^\gamma, \quad \frac{x^\gamma}{\tau(x)} \in L^1([0, A)) \quad \text{for some } \gamma > 0\,,\ A > 0\,,$$
$$\lim_{x\to+\infty} \frac{x\beta(x)}{\tau(x)} = +\infty, \quad \frac{\beta(x)}{\tau(x)} \in L^\infty([0, A)),$$

associated with a couple of technical assumptions.

Several analytical examples are presented in [6] where it appears naturally that $\Lambda(\mathbf{V})$ should be decreasing. Even though no general proof is available as of today, it holds true by continuity when the coefficients do not differ too much from these examples. Also numerics indicate that this property might be true for a large class of transconformation rates $\tau(x)$, including bell-shaped rates, as one can see in Figure 3.

Following [6], the steady states to Equation (1) can now be reformulated in terms of the eigenelements. The so-called 'healthy steady state' corresponds to $(u \equiv 0, v = \overline{V} := \lambda/\gamma)$. More interesting, the 'infectious' steady state (u_∞, V_∞) can exist and corresponds, in Equations (4) and (5), to the relations

$$\Lambda(V_\infty) = 0, \quad u_\infty(x) = \varrho_\infty \mathcal{U}(V_\infty; x), \quad V_\infty = \frac{\lambda}{\gamma + \varrho_\infty \int_0^\infty \tau(x)\mathcal{U}(V_\infty; x)\,\mathrm{d}x}. \tag{6}$$

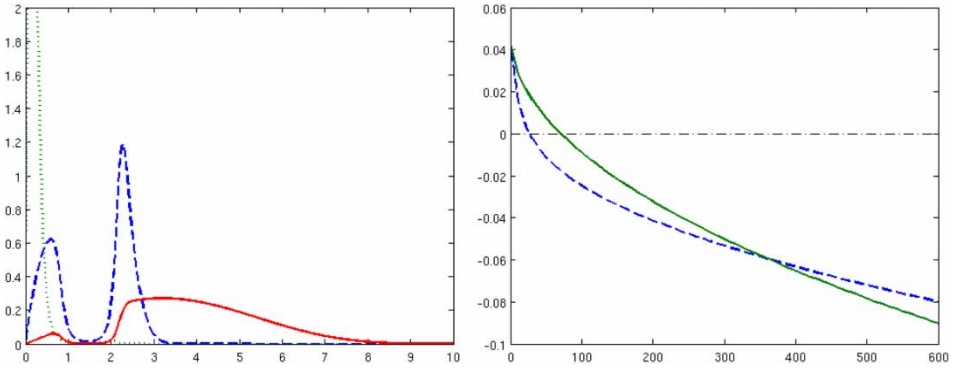

Figure 3. Eigenvalue problem for the microscopic distribution. Left: several eigenfunctions are plotted, for V, respectively, above (full line), below (dotted line), and close to (dashed line) the equilibrium value V_∞. This is the 'constant coefficient' configuration except for the bell-like converting rate $\tau(x)$. Coefficients' values are given in Section 3. Right: numerical computation of the eigenvalue function $\Lambda(V)$ for a bell-like function $\tau(x)$ (dashed line) compared to the 'constant coefficients case', where $\Lambda(V) = \mu_0 - \sqrt{\tau_0\beta_0 V}$ (full line).

Accordingly to the above interpretation, it corresponds to a level of PrPc yielding a zero Malthusian growth for the aggregates, which is an obvious necessary condition for having a stationary state. Furthermore the profile of the size-distribution at equilibrium is given by the eigenfunction $\mathcal{U}(V_\infty; x)$.

Such a steady state only exists if the prion production λ is high enough so as to choose ϱ_∞ which satisfies the third condition, namely

$$V_\infty < \overline{V} := \frac{\lambda}{\gamma}. \tag{7}$$

The question of the stability of these steady states has been extensively studied in the case of 'constant coefficients', i.e., where τ, μ are constant $\beta(x) = \beta_0 x$ and $\kappa(x, y) = 1/y\mathbf{1}_{(0\le x\le y)}$ in [12,15,16,30]. Then the system can be reduced to a three by three system of ordinary differential equations on $(V(t), \int_0^\infty u(x,t)\,\mathrm{d}x, \int_0^\infty xu(x,t)\,\mathrm{d}x)$. It turns out that the condition (7) is sharp and when λ is small only the healthy steady state exists and is stable. If λ is large enough so that the other steady state exists, it is globally attractive. Here, we are interested in non-constant rates.

2.2. *Analysis of stability*

Several stability results are proved in [6]. When λ is small the only steady state to Equation (1) is $(0, \overline{V})$, the healthy state, and it is globally attractive; for any initial data we have $u(t) \to 0$ as $t \to 0$ in L^1. In the case when there is another steady state (u_∞, V_∞), the infectious state, it is proved that trajectories cannot come close to the healthy state (persistency). But it is not known if it is attractive or if other dynamics as periodic solutions can exist.

We complete the result in [6] by removing a size condition on some parameters of the system (see below), and replacing it with an assumption on the global boundedness of the number and mean size of aggregates. The main advantages are twofold: this new criterion has a very clear biological interpretation, and moreover it can be obtained through independent estimates as in Theorem 2.1.

In order to state our new persistency result we first prove a uniform bound

THEOREM 2.1 *Assume that* $\int_0^\infty [1+x]u^0(x)\,\mathrm{d}x < \infty$, $\mu(x) > \underline{\mu} > 0$ *and* $\beta(x) \le \theta\mu(x) + C_\beta x$ *for some constant* $C_\beta \ge 0$ *and* $\theta < 1$, *then the solution* $u(t)$ *to Equation* (1) *is uniformly bounded in* $L^1((1+x)\,\mathrm{d}x)$.

The condition on β involves some smallness and we do not know if it can be improved. However, it is clear that the mortality rate μ should be large enough; otherwise, the constant production of monomers is not balanced by any degradation and the system tends to infinity. On the other hand, the case when $\beta(x)$ has sublinear growth is also of interest and corresponds to a well-established theory, see [10].

Proof We combine the two balance laws (3) and for $a > 0$ to be chosen later on, we calculate

$$\frac{\mathrm{d}}{\mathrm{d}t}\left(V(t) + \int_0^\infty (a+x)u(x,t)\,\mathrm{d}x\right) + \int_0^\infty \big[(a+x)\mu(x) - a\beta(x)\big]u(x,t)\,\mathrm{d}x + \gamma V(t) = \lambda.$$

From our assumption on β, we obtain that

$$\frac{\mathrm{d}}{\mathrm{d}t}\left(V(t) + \int_0^\infty (a+x)u(x,t)\,\mathrm{d}x\right) + \int_0^\infty \big[\big(a(1-\theta)+x\big)\mu(x) - aC_\beta x\big]u(x,t)\,\mathrm{d}x + \gamma V(t) \le \lambda.$$

We now choose a such that $aC_\beta < \underline{\mu}/2$, and we get for some $b > 0$ small enough so that

$$\frac{\mathrm{d}}{\mathrm{d}t}\left(V(t) + \int_0^\infty (a+x)u(x,t)\,\mathrm{d}x\right) + b\left(V(t) + \int_0^\infty (a+x)u(x,t)\,\mathrm{d}x\right) \le \lambda.$$

Thanks to the Gronwall lemma, this differential inequality proves the announced boundedness. ■

Our second result improves the persistency argument in [6] and still uses a duality method based on the weight $\overline{\varphi} = \varphi(\overline{V};\cdot)$. We assume that there are two constants K_1 and K_2 such that

$$\left|\tau(x)\frac{\partial\overline{\varphi}(x)}{\partial x}\right| \le K_1\overline{\varphi}(x) \quad \text{and} \quad \tau(x) \le K_2\overline{\varphi}(x). \tag{8}$$

This condition generally holds true because $\overline{\varphi}$ grows at most linearly at infinity according to general structure properties proved in [24,26,27] and related to Assumption (2).

We have

THEOREM 2.2 *We assume that $\Lambda(\overline{V}) < 0$, $V(0) \le \overline{V}$ and that $\int_0^\infty (1+x)u(t,x)\,\mathrm{d}x$ is uniformly bounded. Then the system remains away from the steady state $(u \equiv 0, \overline{V})$. More precisely we have*

$$\liminf_{t\to\infty} \int_0^\infty \overline{\varphi}(x)\,u(x,t)\,\mathrm{d}x > 0\,.$$

In comparison with [6, Theorem 3], the peculiar size condition on the coefficients, namely $K_1\overline{V} < \Lambda(V) + \gamma$ (where K_1 is introduced in Equation (8), has been removed and replaced by the boundedness of the number and size of the polymers).

Proof For the sake of clarity we introduce the quantities $0 \le v(t) = \overline{V} - V(t) \le \overline{V}$ and $w(t) = \int_0^\infty \overline{\varphi}(x)u(x,t)\,\mathrm{d}x$. Testing the system (1) against $\overline{\varphi}(x)$ (5), it implies after integration by parts

$$\frac{\mathrm{d}}{\mathrm{d}t}v(t) + \gamma v(t) = V(t)\int_0^\infty \tau(x)u(x,t)\,\mathrm{d}x \le \overline{V}K_2 w(t),$$

$$\frac{\mathrm{d}}{\mathrm{d}t}w(t) = -v(t)\int_0^\infty \tau(x)\frac{\partial\overline{\varphi}(x)}{\partial x}u(x,t)\;\mathrm{d}x - \Lambda(\overline{V})w(t) \ge (|\Lambda(\overline{V})| - K_1 v(t))w(t).$$

Note also that $v(t)$ cannot vanish in finite time.

Next we consider for some $\alpha > 1$ to be chosen later on, the quantity $y(t) = w(t)v^{-\alpha}(t)$. It satisfies the differential inequality:

$$\frac{\mathrm{d}}{\mathrm{d}t}\left(\frac{w(t)}{v^\alpha(t)}\right) \ge \frac{w(t)}{v^\alpha(t)}(|\Lambda(\overline{V})| - K_1 v(t)) - \alpha\frac{w(t)}{v^\alpha(t)}\left(-\gamma + \overline{V}K_2\frac{w(t)}{v(t)}\right),$$

and we now choose α large enough so that $\delta = \alpha\gamma + \Lambda(\overline{V}) - K_1\overline{V} > 0$. This leads to the system of differential inequalities:

$$\frac{\mathrm{d}y(t)}{\mathrm{d}t} \ge y(t)\left[\delta - \alpha K_2\overline{V}y^{1/\alpha}w^{1-1/\alpha}\right],$$

$$\frac{\mathrm{d}w(t)}{\mathrm{d}t} \ge w(t)\left[|\Lambda(\overline{V})| - K_1\left(\frac{w}{y}\right)^{1/\alpha}\right]. \tag{9}$$

We denote by $\overline{w} = \limsup_{t\to\infty} w(t)$, which is finite thanks to our global boundness on $u(x,t)$ because $\overline{\varphi}$ has sublinear growth at infinity. Then, the first differential inequality on $y(t)$ tells

us that,

$$\underline{y} := \liminf_{t\to\infty} y(t) \geq \frac{\delta}{(\alpha K_2 \overline{V}\,\overline{w}^{1-1/\alpha})} > 0.$$

And then, we deduce from the second inequality that $\liminf_{t\to\infty} w(t) \geq |\Lambda(\overline{V})|^{\alpha} K_1^{-\alpha} \underline{y}$ and the proof is completed. ■

Note that we need the *a priori* knowledge that $w(t)$ is upper bounded in order to obtain the lower bound from the system (9). And such a property is not a consequence of the dynamics on (y, w) only. This means that some information is lost (as the mortality rate) when reducing the infinite-dimensional system to these two quantities and the upper bound should come from another stage as we mentioned earlier (Theorem 2.1 for instance).

3. Dynamics and strain phenomena

It has been suggested that less stable prion strains are more infectious, as judged by their shorter incubation times [21]. In addition, most infectious particles (fractionnated by sedimentation) seem to be smaller for fast strains than for slow strains [2]. However, how the PrPsc conformation of a specific strain influences its replicative properties remains unclear. In this section, we aim at studying how a slight change in the replicative parameters can reproduce or predict strains properties. We are mainly interested in PrPsc aggregate size distribution, which could be used to study strain mechanisms. Indeed, analysis of the dynamics of model (1) initiated in [6] emphasizes the importance of the size distribution of PrPsc aggregate, which seems to be very informative on prion replication mechanism. Notably, it has been shown that different size repartitions resulting from different replicative parameters can play a role in the strain adaptation mechanism.

Our approach is based both on analysis through the eigenvalue problems (4) and (5) and on direct numerical simulations of the temporal dynamics.

3.1. *Numerics*

Parameters of the nucleated polymerization model for prion growth have been estimated for the 'constant parameters model' from experimental data and are available in the literature, see [15,31] and the references therein. The parameter values used in the sequel have been quoted from Rubenstein *et al*. [31]. Unless explicitly mentioned, they are: $\lambda = 2400$ per day, $\gamma = 4$ per day, $\mu_0 = 0.05$ per day, and $\beta(x) = \beta_0 x$ with $\beta_0 = 0.03$ per day.

The real conversion function is still unknown. We test two different functions, which represent idealized extreme cases:

- a bell-shaped function, accounting for the case of the infectious particles, is concentrated around one specific size. The conversion function $\tau(x)$ is the sum of a basal rate $\tau_0 = 0.001$ and a Gaussian bell centred on m:

$$\tau(x) = \tau_0 + A \exp\left(-(x-m)^2/\sigma^2\right), \tag{10}$$

  with a magnitude A to be chosen by several orders of magnitude above τ_0.
- a sigmoidal shape, when aggregates larger than a critical size are identically more infectious than smaller polymers. Then the conversion function $\tau(x)$ is given by

$$\tau(x) = \tau_0 + A\frac{\exp(x-m)}{1+\exp(x-m)}, \tag{11}$$

  with a magnitude A to be chosen by several orders of magnitude above τ_0.

Throughout the rest of this paper, the simulations assume an initial PrPc population $V(0) = \overline{V} = \lambda/\gamma$ (corresponding to the healthy steady state because we assume inoculation in an healthy animal) and an initial PrPsc distribution which is a small perturbation of the zero steady state, given by $u(x, 0) = 0.5x^2/(1 + x^4)$.

3.2. *Effects of the conversion rate*

Differently shaped size repartition of the conversion rate greatly affects the PrPsc aggregates size distribution [6]. We test here the situation where changes in conformation do not lead to a completely different profile of converting activity, but only a change of either the magnitude of the conversion or the location of the most infectious particles. For the experiments depicted in Figures 4 and 5, varying parameters act upon the kinetics of PrPsc accumulation as follows: the higher the transconformation rate are or the smaller the most converting particles are, the faster the PrPsc accumulates, and thus, the shorter the incubation time seems to be. In particular, this implies that a fast strain could be able to fix and transconform PrPc either with great efficiency or by smaller aggregates (or both). Interestingly, our simulations also predict changes in the size-distribution of PrPsc, whose variations are specific of the varying parameters.

In the case of a bell-shaped conversion rate, we also have tested the effect of the tightness of the converting peak, by studying the dominant eigenvalue. Indeed, when we focus on the exponential growth of PrPsc (as is the case in the brain but corresponds only to the early stages of accumulation in the spleen), the eigenvalue problem can be used during the initial phase of

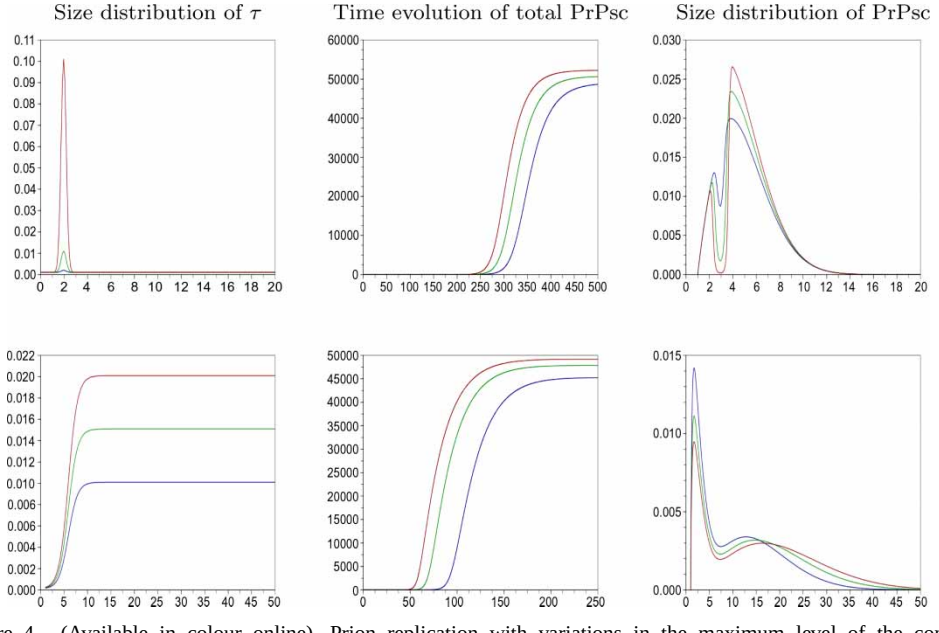

Figure 4. (Available in colour online). Prion replication with variations in the maximum level of the conversion rate τ. Transconformation rates are given by (top) $\tau_1(x) = 0.001 + H * \exp(-10 * (x-2)^2)$. Three values for H have been tested : $H = 0.001$ (blue line), $H = .01$ (green line) and $H = 0.1$ (brown line) (bottom) $\tau_2(x) = 0.0001 + G\exp(x-5)/(1+\exp(x-5))$. Three values for G have been tested : $G = 0.01$ (blue line), $G = .015$ (green line) and $H = 0.02$ (brown line). Left: size distribution of τ_1 and τ_2 (abscissa = PrPsc aggregates size; ordinate = rate τ). Middle: time evolution of total PrPsc for : (B1) τ_1 and (B2) τ_2. (abscissa = Time (in day) ; ordinate = rate τ (per day). Right: normalized PrPsc aggregates size distribution at t1 = 90 days and t2 = 20 days, corresponding to the exponential growth of PrPsc. The distributions are normalized by the total number of PrPsc aggregates (abscissa = PrPsc aggregates size; ordinate = PrPsc aggregates number).

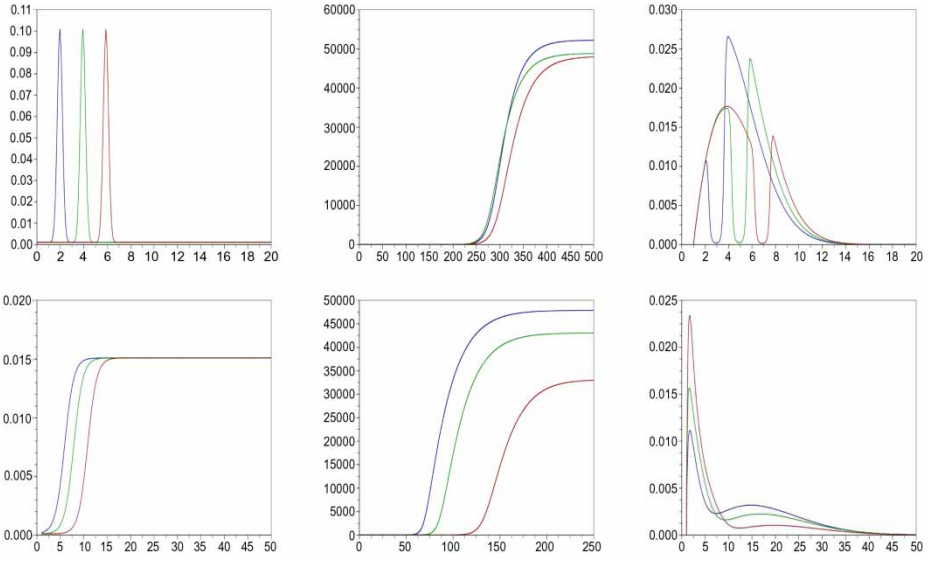

Figure 5. (Available in colour online). Prion replication with variations in the locus of the conversion rate τ. Transconformation rates are given by: (top) $\tau_1(x) = 0.001 + 0.1 * \exp(-10 * (x - m)^2)$. Three values for m have been tested : $m = 2$ (blue line), $m = 4$ (green line) and $m = 6$ (brown line) (bottom) $\tau_2(x) = 0.0001 + 0.015\exp(x - l)/(1 + \exp(x - l))$. Three values for l have been tested : $l = 5$ (blue line), $l = 7$ (green line) and $l = 10$ (brown line) Left, Middle and Right: Same as Figure 4.

exponential growth (occurring at least in the diseased brains). We assume below that $\overline{V} > V_\infty$ according to Equation (7), that $\Lambda(V)$ is a decreasing function so that instability of the healthy state holds true as proved in [6]. This holds for the choice of coefficients mentioned above. We may assume that $V(t)$ remains close enough to $\overline{V}$ because $u(x, t)$ dynamics undergoes an exponential growth phase, while the polymerization behaves following a linear problem. Actually the second equation in (1) is decoupled from the first one at the first order of approximation. The dominant eigenvalue $-\Lambda(\overline{V})$ thus measures the exponential growth of the PrPsc total population (see [26] for a mathematical formulation of this fact using the generalized relative entropy). Several transconformation rates $\tau(x)$ – being the same basal rate τ_0 combined with a more and more concentrated Gaussian bell are tested – and the corresponding growth rate in the exponential phase $-\Lambda(\overline{V})$ are computed numerically (Figure 6). Interestingly, the results exhibit a best compromise around $\alpha \approx 0.01$ (intermediate concentrations of the peak). Thus, according to this model the optimal conditions for PrPsc accumulation in the exponential expansion phase do not correspond to a very thin peak.

3.3. *Effects of the fragmentation rate*

As suggested in [21,33], prion strains can differ in their stability. Here, we make the assumption that the stability of a strain is only represented by the framentation rate β. However, it could also be interesting to study the effect of the degradation rate μ. According to numerical experiment depicted in Figure 7, increasing the fragmentation rate leads to a faster PrPsc accumulation for a bell-shaped converting rate τ as for a sigmoidal τ. However, for a sigmoidal τ with a higher critical threshold, the inverse effect is observed, due to the fact that small aggregates are less able to convert PrPc than larger PrPsc polymers, and then multiplying the number of small particles does not compensate for the loss of conversion activity any more. Surprisingly enough, we also can observe that when the fragmentation accelerates the accumulation of PrPsc, this faster accumulation leads to a lower level of total PrPsc amount at the plateau.

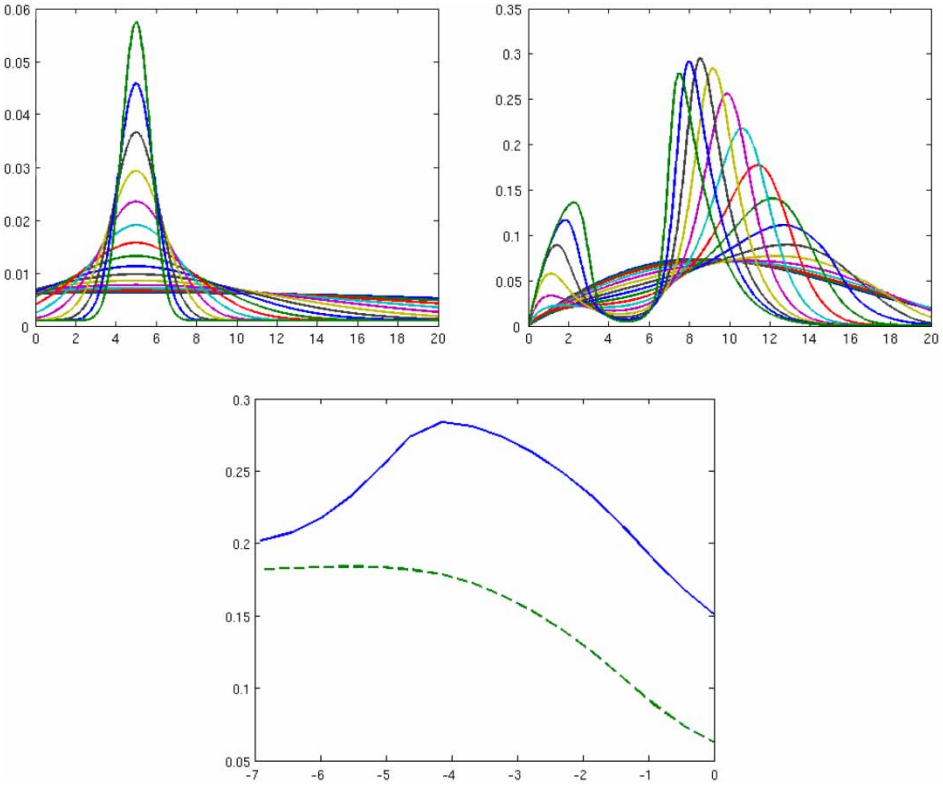

Figure 6. Influence of the transconformation tightness (top) The transconformation rate with several levels of concentration: $\tau(x) = \tau_0 + \alpha\varphi(\alpha(x-m))$, where φ is a Gaussian function and $\alpha = 10^{(-3:.2:0)}$). (middle) The corresponding eigenfunctions $\mathcal{U}(\overline{V}; x)$. (bottom) The exponential growth rate $-\Lambda(\overline{V})$ (solid line) as a function of α (logarithmic scale, units for $-\Lambda(\overline{V})$ are day^{-1}) and the effective transconformation rate (dashed line) $\tau_{\text{eff}} = \int \tau(x)\mathcal{U}(\overline{V}, x)\,\mathrm{d}x$ (magnified 30 times). Bimodal distribution begins for $\ln(\alpha) \gtrsim -3$ and thus does not correspond to the distribution having the best Malthusian parameter.

4. Conclusion and perspectives

We have continued the analysis in [6] concerning size-dependent polymerization rates in the standard model (1) for prion PrPsc self-replication. The interesting situation is when the prion production rate is large enough to permit an infectious steady state. Analytical study of its instability remains an open problem (see [12,15,16,30] for the 'constant coefficients' case) but we could improve a previous result showing that the healthy state is unstable and solutions remain globally bounded. As previously but in a more general framework, we confirm that the amount of PrPc is critical for the development of prion diseases. This is in accordance with well-known experimental results, where PrP-KO mice cannot be infected [5]. However, this result may have wider implications for many other neurodegenerative diseases. Indeed, numerous pathologies (such as Alzheimer's disease, Parkinson's disease and Hungtington's disease) are characterized by the aberrant polymerization and accumulation of misfolded proteins. Many evidences show that they can be induced in transgenic models (see [35,37] for a review). Thus, whether these misfolding protein disorders are transmissible or not is currently widely debated. Our results suggest that the bioavailability of the amyloid precursor is critical for transmissibility. This is consistent with the fact that, in prion diseases, prion precursor is the protein itself and naturally present in large amount in neurons, whereas in Alzheimer's disease, Abeta is only a minor proteoteolytic cleavage product of the amyloid precursor protein (APP).

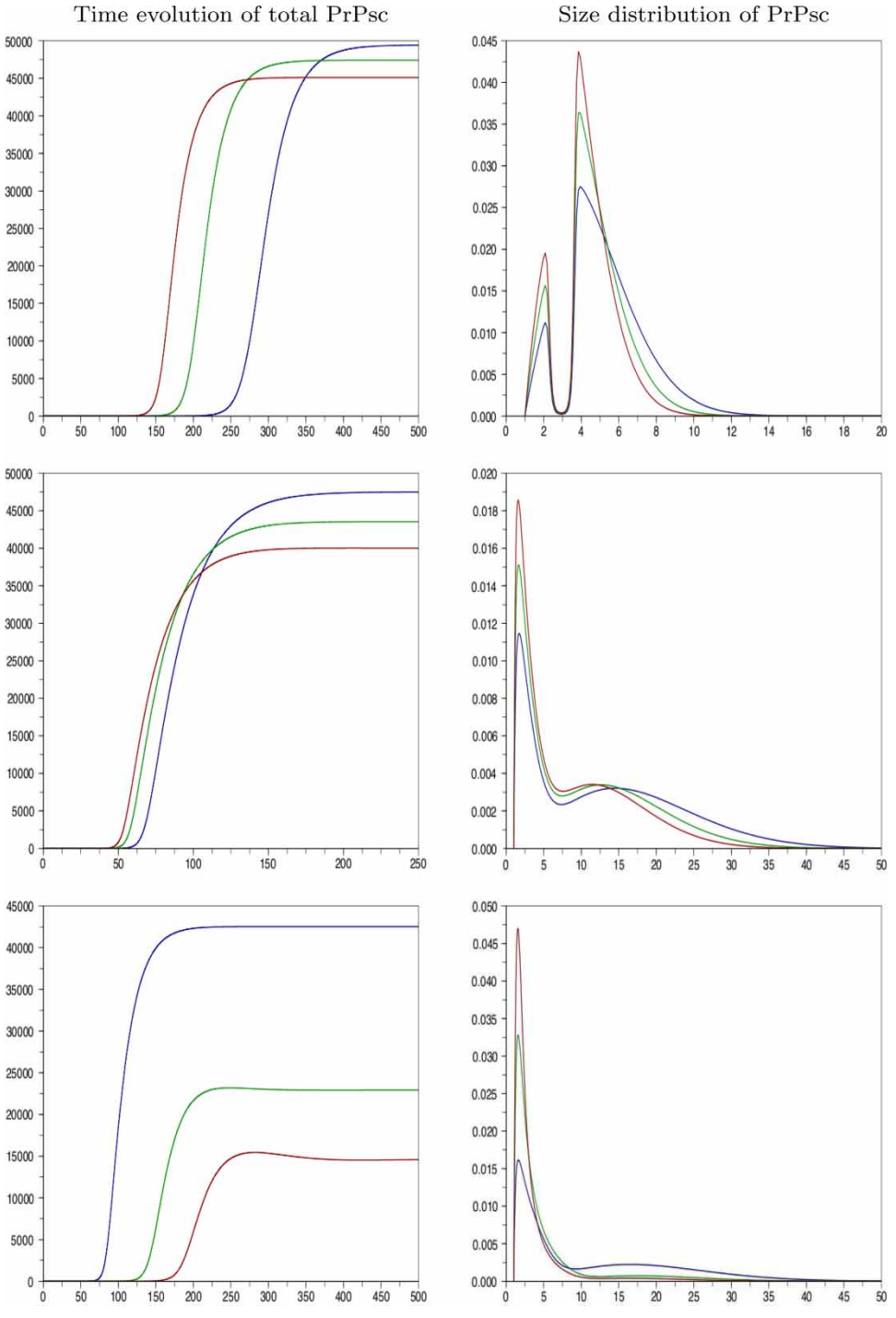

Figure 7. (Available in colour online). Prion replication with variations in the fragmentation rate of aggregates. Three values for β have been tested ($\beta = 0.0314$ - blue line, $\beta = 0.0471$ - green line and $\beta = 0.0628$ - brown line) for three conversion rates $\tau_1(x) = 0.001 + 0.1\exp\left(-10(x-2)^2\right)$ (top), $\tau_2(x) = 0.0001 + 0.015\exp(x-5)/1 + \exp(x-5)$ (middle) and $\tau_3(x) = 0.0001 + 0.015\exp(x-10)/1 + \exp(x-10)$ (bottom) (Left) Time evolution of total PrPsc (abscissa = Time (in day) ; ordinate = PrPsc total amount) (Right) Normalized PrPsc aggregates size distribution at t1 = 96 days (for τ_1), t2 = 20 days (for τ_2) and t3 = 60 days (for τ_3) corresponding to the exponential growth of PrPsc. The distributions are normalized by the total number of PrPsc aggregates (abscissa = PrPsc aggregates size; ordinate = PrPsc aggregates number).

This necessary condition of PrPc bioavaibility is, however, insufficient to explain strain mechanisms, since species expressing PrPc can be infected only by specific strains. Thus additional constraints are likely to be required for prion strain transmission and propagation. Such constraints can be purely physicochemical, due to one peculiar structure of prion aggregates. Indeed, a large body of literature suggests that differences between prion strains lie in the diversity of structures of PrPsc aggregates that can be stably and faithfully propagated [1,7,8,21,25,32,36]. However, it remains poorly understood how these changes in the conformation of PrPsc aggregates can account for their physiopathological effects and their relationship with the host [21]. Although our model does not separate the host contribution from the strain contribution, it represents on the contrary the relationship between host and pathogen and it allows studying which elementary replicative parameter is critical in strain propagation.

Among the attempted biochemical characterization of prion strains, a relationship was found between the relative stability values of PrPsc aggregates [21] or level of aggregation [32] and incubation times, indicating that less stable prions are more infectious, as judged by their shorter incubation times. This is presumably because unstable prions fragment more easily, giving rise to smaller aggregates of PrPsc that are more infectious than larger ones. Our model agrees with these observations for a bell-shaped conversion rate, since increasing the fragmentation rate β_0 leads to a faster PrPsc accumulation. Inverse results can be obtained for some sigmoidal conversion rates. It does not immediately mean that a sigmoidal conversion rate is unrealistic, since this result strongly depends on the size distribution of the fragmentation rate. However, it emphasizes the need for precisely monitoring the fragmentation rate, which might depend on the PrPsc aggregate size in a more complex manner than the linear dependence supposed here.

We have also investigated the implications of varying the conversion rate: do different strain conformations lead to a more efficient fixation and conversion by the same aggregates or do they lead to different most converting particles? Our numerical simulations alone do not answer to this question, but interestingly, they show that whereas changing parameters leads to similar effects on PrPsc accumulation kinetics, the resulting size-distribution variations are different. Thus the achievement of experimental size-distribution of PrPsc aggregates for many prion strains could therefore allow to better understand the molecular mechanisms involved in prion strain phenomenon.

To conclude, this work completes the study initiated in [6], notably in studying strain phenomenon. It emphasizes the potential role of PrPsc aggregates size distribution, which could be a signature of prion strain converting abilities. The next step of our work is to approximate faithfully the inverse problem in order to obtain the size dependence of the transconformation rate from the distribution of PrPsc for several strains. This knowledge is a critical step for experimental approaches of prion infectivity investigation like PMCA. Indeed, we have observed several times the existence of an optimal converting rate for PrPsc accumulation (see for instance the tightness in the case of a bell-shaped converting rate), which means that only slight changes in the replicative parameters can dramatically influence the kinetics of PrPsc accumulation. It could explain the sensitivity of PMCA to experimental procedures. Complete understanding of how the PrPsc accumulation of a given strain depends on their replicative parameters could help to optimize strain-specific PMCA protocols.

References

[1] A. Aguzzi, *Unravelling prion strains with cell biology and organic chemistry*, Proc. Natl. Acad. Sci. USA 105 (2008), pp. 11–12.
[2] V. Beringue, Oral communication, Neuroprion Congress, Madrid 2008.
[3] V. Beringue, K.T. Adjou, F. Lamoury, J.P. Deslys, R. Race, and D. Dormont, *Opposite effects of dextran sulfate 500, the polyene antibiotic MS-8209, and Congo red on accumulation of the protease-resistant isoform of PrP inthe spleens of mice inoculated intraperitoneally with the scrapie agent*, J. Virol. 74 (2000), pp. 5432–5440.

[4] M. Bruce, A. Chree, I. McConnell, J. Foster, G. Pearson, and H. Fraser, *Transmission of bovine spongiform encephalopathy and scrapie to mice: strain variation and the species barrier*, Phil. Trans. R. Soc. Lond. B 343 (1994), pp. 405–411.

[5] H. Bueler, A. Aguzzi, A. Sailer, R.A. greiner, P. Autenried, M. Aguet, and C. Weissmann, *Mice devoid of PrP are resistant to scrapie*, Cell 369 (1993), pp. 139–1347.

[6] V. Calvez, N. Lenuzza, D. Oelz, J.-Ph. Deslys, P. Laurent, F. Mouthon, and B. Perthame, *Size distribution dependence of prion aggregates infectivity*, Math Biosci. 217 (2009), pp. 88–99.

[7] N.J. Cobb and W.K. Surewicz, *Prion strains under the magnyfying glass*, Nat. Struct. Mol. Biol. 14 (2007), pp. 882–884.

[8] J. Collinge and A.R. Clarke, *A general model of prion strains and their pathogenicity*, Science 318 (2007), pp. 930–936.

[9] J. Collinge, M.S. Palmer, K.C. Sidle, A.F. Hill, I. Gowland, J. Meads, E. Asante, R. Bradley, L.J. Doey, and P.L. Lantos , *Unaltered susceptibility to BSE in transgenic mice expressing human prion protein*, Nature 378 (1995), pp. 779–783.

[10] M. Doumic and P. Gabriel, *Analysis of a fragmentation model arising in prion aggregation*. Work in preparation.

[11] M. Doumic, Th. Goudon, and Th. Lepoutre, *Scaling limit of a discrete prion dynamics model*. Work in preparation.

[12] H. Engler, J. Pruss, and G.F. Webb, *Analysis of a model for the dynamics of prions II*, J. Math. Anal. Appl. 324 (2006), pp. 98–117.

[13] M. Escobedo, P. Laurençot and S. Mischler, *Fast reaction limit of the discrete diffusive coagulation–fragmentation equation*, Comm. Partial Differential Equations 28 (2003), pp. 1113–1133.

[14] H. Fraser and A.G. Dickinson, *Agent-strain differences in the distribution and intensity of grey matter vacuolation*, J. Comp. Path. 83 (1973), pp. 29–40.

[15] M.L. Greer, L. Pujo-Menjouet, and G.F. Webb, *A mathematical analysis of the dynamics of prion proliferation*, J. Theoret. Biol. 242 (2006), pp. 598–606.

[16] M.L. Greer, P. Van den Driessche, L. Wang, and G.F. Webb, *Effects of general incidence and polymer joining on nucleated polymerization in a model of prion proliferation*, SIAM J. Appl. Math. 68 (1) (2007), pp. 154–170.

[17] R.H. Kimberlin and C.A. Walker, *Incubation periods in 6 models of intraperitoneally ijected scrapie depend mainly on the dynamics of agent replication within the nervous system and not the lymphoreticular system*, J. Gen. Virol. 369 (1988), pp. 2953–2960.

[18] P. Laurençot and S. Mischler, *From the discrete to the continuous coagulation–fragmentation equations*, Proc. Roy. Soc. Edinburgh Sect. A 132 (2002), pp. 1219–1248.

[19] P. Laurençot and C. Walker, *Well-posedness for a model of prion proliferation dynamics*, J. Evol. Equations 7 (2007), pp. 241–264.

[20] G. Legname, I.V. Baskakov, H.-O.B. Nguyen, D. Riesner, F.E. Cohen, S.J. DeArmond, and S.B. Prusiner, *Synthetic mammalian prions*, Science 305 (2004), pp. 673–676.

[21] G. Legname, H-O.B. Nguyen, D. Peretz, F.E. Cohen, S.J. DeArmond, and S.B. Prusiner, *Continuum of prion protein structures enciphers a multitude of prion isolate-specified phenotypes*, Proc. Natl. Acad. Sci. USA 103 (2006), 19105–19110.

[22] J. Masel, V. Jansen, and M. Nowak *Quantifyng the kinetic parameter of prion replication*, Biophys. Chem. 77 (1999), pp. 139–152.

[23] P. Michel, *Existence of a solution to the cell division eigenproblem*, Math. Models Methods Appl. Sci. 16 (2006), pp. 1125–1153.

[24] P. Michel, S. Mischler, and B. Perthame, *General relative entropy inequality: an illustration on growth models*, J. Math. Pures Appl. 84 (2005), pp. 1235–1260.

[25] R. Morales, K. Abid, and C. Soto, *The prion strain phenomenon: molecular basis and unprecedented features*, Biochim. Biophys. Acta 1772 (2007), pp. 681–691.

[26] B. Perthame, *Transport Equations in Biology*, Frontiers in Mathematics, Birkhäuser, Basel, 2007.

[27] B. Perthame and L. Ryzhik, *Exponential decay for the fragmentation or cell-division equation*, J. Differential Equations 210 (2005), pp. 155–177.

[28] S.B. Prusiner, M. Scott, D. Foster, K.-M. Pan, D. Groth, S.-L. Yang, D. Serban, G.A. Carlson, P.C. Hoppe, D. Westaway, and S.J. DeArmond, *Transgenic studies implicate interactions between homologous PrP isoforms in scrapie prion replication*, Cell 63 (1990), pp. 673–386.

[29] S.B. Prusiner, M.R. Scott, S.J. DeArmond, and F.E. Cohen, *Prion protein biology*, Cell 93 (1998), pp. 337–348.

[30] J. Pruss, L. Pujo-Menjouet, G.F. Webb, and R. Zacher, *Analysis of a model for the dynamics of prions*, Discrete Cont. Dyn. Sys. Ser. B 6(1) (2006), pp. 215–225.

[31] R. Rubenstein, P.C. Gray, T.J. Cleland, M.S. Piltch, W.S. Hlavacek, R.M. Roberts, J. Ambrosiano and J.-I. Kim, *Dynamics of the nucleated polymerization model of prion replication*, Biophys. Chem. 125 (2007), pp. 360–367.

[32] C.J. Sigurdson, K.P.R Nilsson, S. Hornemann, G. Manco, M. Polymenidou, P. Schwarz, M. Leclerc, P. Hammarstrom, K. Wuthrich and A. Aguzzi, *Prion strain discrimination using luminescent conjugated polymers*, Nat. Methods 4 (2007), pp. 1023–1030.

[33] J.R. Silveira, G.J. Raymond, A.G. Hughson, E.R. Richard, V.L. Sim, S.F. Hayes and B. Caughey, *The most infectious prion protein particles*, Nature 437 (2005), pp. 257–261.

[34] G. Simonett and C. Walker, *On the solvability of a mathematical model for prion proliferation*, J. Math. Anal. Appl. Vol. 324 (1) (2006), pp. 580–603.

[35] C. Soto and L.D. Estrada *Protein misfolding and neurodegenration*, Arch. Neurol. 65 (2008), pp. 184–189.

[36] A.M. Thackray, L. Hopkins, M.A. Klein, and R. Budjoso, *Mouse-adapted ovine scrapie prion strains are characterized by diferent coformers of PrPsc*, J. Virol. 81 (2007), 12119–12127.
[37] L.C. Walker, H. Levine, M.P. Mattson, and M. Jucker *Inducible proteopathies*, Trends Neurosci. 29 (2006), 438–443.
[38] P. Weber, A. Giese, N. Piening, G. Mitteregger, A. Thomzig, M. Beekes, and H.A. Kretzschmar, *Generation of genuine prion infectivity by serial PMCA*, Vet. Microbiol. 123 (2007), pp. 346–357.
[39] P. Weber, L. Reznicek, G. Mitteregger, H. Kretzschmar, and A. Giese, *Differential effects of prion particle size on infectivity in vivo and in vitro*, Biochem. and Biophy. Res. Comm. 369 (2008), pp. 924–928.